Magnetic Control of Optical Spatial Solitons

A. D. Boardman and K. Xie
Joule Laboratory, Department of Physics, University of Salford, England, M5 4WT United Kingdom
(Received 30 March 1995)

Calculations involving the propagation of a pair of bright, spatial solitons in magneto-optic waveguides are presented. It is shown that an external magnetic field can force bright solitons from a state of attraction to each other into isolation from each other. It is also shown that TE-TM conversion, a typical magneto-optic phenomenon, can be controlled by the input power. Finally, an elegant Hamiltonian analysis of the critical points of the phase space is used to prove that various stable, or unstable, regimes can be established.

PACS numbers: 42.50.Rh

It has long been asserted in the literature that optical-magnetostatic wave interactions ought to be competitive with the commercially available acousto-optic devices [1], with the added advantages of higher ($\cong$20 GHz) operation coupled to tunability supplied by the applied magnetic field. This tunable magneto-optic effect has never been introduced into nonlinear optics, so this paper breaks new ground in this respect. Experimental verification of the results predicted here should be within reach, because garnet films are now the products of a mature fabrication technology. Indeed exploiting magneto-optical properties will produce impressive integrated optical units [1], when compared to those based upon GaAs or $LiNbO_3$ technologies. In view of this development, it is exciting to investigate integrated optical device possibilities that use not only magneto-optic interactions but nonlinearity as well. Even now, molecular beam epitaxy permits the growth of magnetic garnets onto GaAs and other III-V materials. Also yttrium iron garnet (YIG) is transparent [1] at $\cong 1.1\ \mu$m, so the operational wavelength is also attractive. Figure 1 shows the waveguide structure under investigation. The propagation of the electromagnetic beams is along the z direction, confinement by *weak* guiding occurs in the $\pm y$ directions, and nonlinearly constrained diffraction [2–4] takes place in the plane of the nonlinear film, in the $\pm x$ directions. The waveguide structure consists of a plane nonlinear, nonmagnetic film, bounded by semi-infinite (thick), identical, longitudinally magnetized magneto-optic material that has a dielectric function [5]

$$\varepsilon_m = \begin{bmatrix} n_m^2 & -iQn_m^2 & 0 \\ iQn_m^2 & n_m^2 & 0 \\ 0 & 0 & n_m^2 \end{bmatrix}, \qquad (1)$$

where n_m is the linear refractive index of the magneto-optical material. In the system selected here, the electric field components E_x and E_y couple to each other through the parameter Q. Since the waveguide is weakly guiding, the longitudinal electric field component E_z satisfies the inequality $|E_z| \ll |E_x|, |E_y|$, so this is the best case to choose for the moment. More strongly guiding situations can be envisaged in future investigations, however, for which the polar (E_x coupled to E_z) or transverse (E_y coupled to E_z) magneto-optic cases will be just as important. The part of the waveguide structure that becomes nonlinear is assumed to develop a Kerr type of nonlinearity so that the third-order nonlinear polarization has the following x and y components [3,4]:

$$P_{x,y}^{(3)} = \varepsilon_0 \alpha [(|E_x|^2 + |E_y|^2) E_{x,y} \pm f(E_x^* E_y - E_x E_y^*) E_{y,x}], \qquad (2)$$

where $f = 4\chi_{yxyx}/\chi_{xxxx}$, $\alpha = \frac{3}{4}\chi_{xxxx}$, and χ_{ijkl} is the familiar fourth-rank tensor describing the nonlinearity. Note $f = 0, \frac{1}{3}, 1$ for thermal, electronic distortion, or molecular orientational nonlinear mechanisms, respectively. If x, y, z are measured in units of ω/c, ω is the angular frequency and c is the velocity of light in vacuo, the electric field vector is $\mathbf{E} = (E_x, E_y)e^{-i\omega t}$, then the equation for $E_{x,y}$ is

$$\nabla^2 E_j + (n^2 + \Delta n_j^2) E_j = 0, \qquad j = x, y, \qquad (3)$$

where Δn_j are the perturbations to the linear refractive index n in various parts of the waveguide structure. From Eqs. (1) and (2)

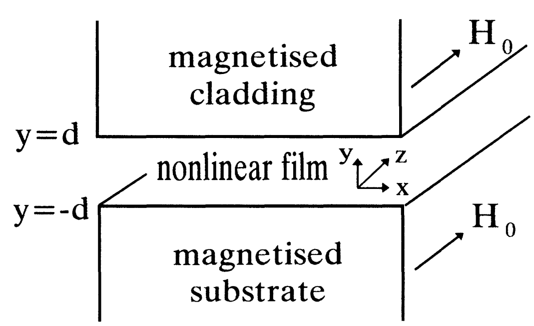

FIG. 1. The waveguide structure. H_0 is the applied magnetic field needed to activate the magneto-optic material. Both the cladding and substrate are semi-infinite.

0031-9007/95/75(25)/4591(4)$06.00

$$\Delta n_x^2 = \begin{cases} \alpha\left[|E_x|^2 + |E_y|^2 + f\left(\frac{E_x^*}{E_x} E_y^2 - |E_y|^2\right)\right], & |y| < d, \\ -iQ\left[\frac{1}{E_x}\frac{\partial^2 E_y}{\partial x^2} - \frac{1}{E_x}\frac{\partial^2 E_x}{\partial x \partial y} + n_m^2 \frac{E_y}{E_x}\right], & |y| > d, \end{cases} \quad (4)$$

with a corresponding form for Δn_y. In Eqs. (3) and (4), the electric field components are $E_{x,y} = \Gamma A_{x,y}(y) B_{x,y}(x,y) \exp(i\omega\beta z/c)$, where β is a common effective index, $A_{x,y}(y)$ are the *unperturbed* modal fields, Γ is a normalization factor, and $B_{x,y}$ are slowly varying amplitudes. After applying standard, first-order, perturbation theory [3,4], the evolution equation for B_x is

$$i2\beta \frac{\partial B_x}{\partial z} + \frac{\partial^2 B_x}{\partial x^2} + 2\nu B_x - iQ_4 \frac{\partial^2 B_y}{\partial x^2} + iQ_2 \frac{\partial B_x}{\partial x} - iQ_1 B_y + \alpha'[(|B_x|^2 + |B_y|^2)B_x + f(B_x^* B_y - B_x B_y^*)B_y] = 0, \quad (5)$$

with

$$Q_1 = n_m^2 Q \frac{\int_{-\infty}^{-d} A_x A_y \, dy + \int_d^{+\infty} A_x A_y \, dy}{\int_{-\infty}^{+\infty} A_x^2 \, dy}, \quad Q_2 = \frac{A_x^2(\pm d) Q}{\int_{-\infty}^{+\infty} A_x^2 \, dy}, \quad Q_3 = \frac{\int A_y (\partial^2 A_x / \partial y^2) \, dy}{\int A_y^2 \, dy},$$

$$Q_4 = \frac{Q_1}{n_m^2}, \quad \nu = \frac{\beta_x^2 - \beta_y^2}{4}, \quad \alpha' = \alpha \frac{\int_{-\infty}^{+\infty} |A_x|^4 \, dy}{(\int_{-\infty}^{+\infty} |A_x|^2 \, dy)^2}.$$

There is also an equation for B_y in which parameters Q_3, Q_2, and Q_1 appear. Note that $\beta_{x,y}$ are the wave numbers of the solution of the *unperturbed* TE, TM equations so that ν is a birefringence parameter. It is not difficult to get expressions for the linear modal field distributions A_x and A_y and to show that $A_x \cong A_y$, for any typical data.

For a spatial soliton beam of natural width D_0, the diffraction length is $L_D = 2\beta D_0^2 \omega / c$, so z will be scaled with L_D and x will be scaled with D_0, i.e., the transformations $x \longrightarrow D_0 x'$, $z \longrightarrow L_D z'$ will be affected. The post-scaling factors in Eq. (5) are $(\omega^2/c^2) D_0^2 Q_1$, Q_4, $(\omega^2/c^2) D_0^2 \nu$, and $(\omega/c) D_0 Q_2$. Typically [2–4], $L_D \cong 2.2$ mm, $D_0 \cong 8.5$ μm, and $Q \cong 1 \times 10^{-4}$ so that, for a wavelength of interest, $(\omega^2/c^2) D_0^2 Q_1 \cong 0.4$, $Q_4 \cong 10^{-4}$, $(\omega^2/c^2) D_0^2 \nu \cong 0.1$, and $(\omega/c) D_0 Q_2 \cong 10^{-2}$. Hence only the magneto-optic term involving Q_1 and the birefringence term involving ν are of any significance. Even then, the birefringence term is a consequence of waveguide design and can be designed out of the problem, if it is so desired. A nonlinear length $L_{\rm NL} = (4\beta c/\alpha'\omega)[\text{amplitude}]^{-2}$ can also be used and a final transformation $\psi_{1,2} = N B_{x,y}$ can be made, where $N = \sqrt{L_D / L_{\rm NL}}$. After dropping the dashes on x and z, for ease of notation, and adopting the definitions $(\omega^2/c^2) D_0^2 Q_1 \longrightarrow Q_1$, $(\omega^2/c^2) D_0^2 \nu \longrightarrow \nu$ this nonlinear magneto-optic problem can be formulated in terms of the coupled equations ($j = 1, 2$)

$$i \frac{\partial \psi_j}{\partial z} + \frac{\partial^2 \psi_j}{\partial x^2} + 2(|\psi_1|^2 + |\psi_2|^2)\psi_j \pm 2f(\psi_1^* \psi_2 - \psi_1 \psi_2^*)\psi_3 \pm 2\nu \psi_j \mp iQ_1 \psi_{3-j} = 0. \quad (6)$$

There are many distributions experimentally possible for Q_1. For instance, the simplest form is $Q_1(x) = \text{const}$, but, more generally, it is also possible to have $Q_1(-x) = Q_1(x)$, or $Q_1(-x) = -Q_1(x)$, where $Q_1(x)$ is a *periodic* function of x. Such periodicity could be created by making a magneto-optic layer from magnetized domains that are alternating in sign (magnetization direction). At this stage the Q_1 that is used in Eq. (5) has been transformed to $(\omega^2/c^2) D_0^2 Q_1$ for use in Eq. (6). Specifying Q_1, therefore, implies a choice of ω, D_0, n_m, Q, and $2d$, the waveguide thickness. As stated earlier, Q is typically 10^{-4} for YIG, and that material has a saturation magnetization of 1750 G. It is also important to remember that this theory applies to single mode waveguides, for which the thickness will be the order of 2 μm.

Figure 2 shows an example of the magneto-optic effect for the case when $\nu = 0$ and there are two beams that are, initially, in phase. For $Q_1 \neq 0$, it is well known that two in-phase solitons will be trapped by each other. Figure 2, however, shows what happens to this interaction if an applied magnetic field is switched on. For this example, $Q_1 = -0.4 \sin(\pi x/2)/|\sin(\pi x/2)|$, i.e., a periodic square function. Collision is shown to be prevented. In effect, the magnetic field creates a potential well in which the beam can be located. A closer inspection reveals that the output beams are mixtures of TE and TM polarizations, even though the initial polarization is purely TE or TM. This TE-TM conversion possibility is well known in linear magneto-optics, but nonlinearity changes the length scale and, consequently, changes the rate of TE-TM conversion. Figure 3 shows a simpler way in which this conversion can proceed for *constant* Q. Initially there is only TE polarization and there is no TM polarization. At a certain propagation distance L, all the TE energy is

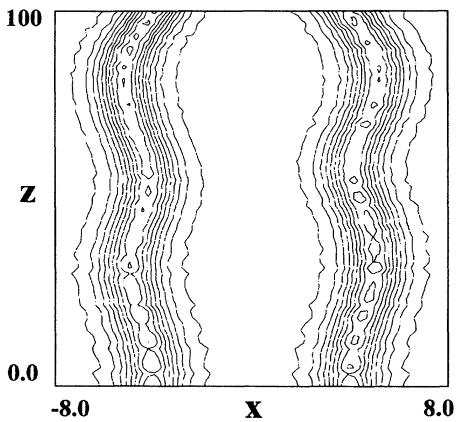

FIG. 2. Interaction of two solitons: $\psi_1 = \operatorname{sech}(x - 4)$, $\psi_2 = \operatorname{sech}(x + 4)$, under the influence of an applied magnetic field. $Q_1 = -0.4\sin(\pi x/2)/|\sin(\pi x/2)|$ and $\nu = 0$.

converted into the TM mode. After propagating another distance L all the energy is converted back to TE again. This pattern is repeated, periodically, every $2L$. In fact, an analytic estimate of the period $2L$ can be rather easily obtained from a variational principle [3,4,6]. For simplicity, it will be applied here under the assumption that the beam width is a constant during the process of conversion. This assumption has been previously used [6] and has been proved to give good qualitative results. This assumption is also supported by Fig. 3, which contains the true polarization dynamics of the beams. The behavior of the beams can be represented quite well, therefore, by choosing the trial functions $\psi_1 = \eta_1 \operatorname{sech}(x)\exp(i\theta_1)$ and $\psi_2 = \eta_2 \operatorname{sech}(x)\exp(i\theta_2)$, where η_1, η_2 are amplitudes of the TE and TM waves and θ_1, θ_2 are their respective phases. The beam widths are normalized to unity. Following the same variational technique as Ref. [6] the two evolution equations for the phase and amplitude differences are

$$\frac{dU}{d\zeta} = \tfrac{8}{3} f(1 - U^2)\sin\theta\cos\theta - Q_0\sqrt{1 - U^2}\cos\theta\,, \tag{7}$$

$$\frac{d\theta}{d\zeta} = \tfrac{8}{3} fU\sin^2\theta - Q_0\frac{U}{\sqrt{1 - U^2}}\sin\theta\,, \tag{8}$$

where $\theta = \theta_2 - \theta_1$, $\eta_1^2 + \eta_2^2 = \text{const}$, $U = (\eta_2^2 - \eta_1^2)/(\eta_2^2 + \eta_1^2)$, $\zeta = (\eta_2^2 + \eta_1^2)z$, and $Q_0 = \frac{1}{(\eta_2^2+\eta_1^2)}\int_{-\infty}^{+\infty} Q_1 \times \operatorname{sech}^2 x\, dx$. If a pure TM wave is launched at the input $[\eta_1(\zeta = 0) = 0,\ \eta_2(\zeta = 0) = 1]$, a simple solution to the coupled evolution equation is $\eta_2^2 = \cos^2(Q_0\zeta/2)$, $\eta_1^2 = \sin^2(Q_0\zeta/2)$. These functions repeat at $Q_0\zeta_0 = 2\pi$. The periodic length z_0 is therefore $z_0 = 2\pi/\int_{-\infty}^{+\infty} Q_1 \operatorname{sech}^2 x\, dx$. Note z_0 is power dependent because it is important to realize in this formulation that Q_1 is, effectively, $(\omega^2/c^2)D_0^2 Q_1$. Hence a change in the input beam width D_0 causes the period of the TE-TM conversion to change. Accordingly, a polarization filter, placed at the end of the waveguide, will see a variation in the output. Since the beam width and the total power of a spatial soliton bear a certain relationship to each other, a polarization conversion device, continuously tunable by the total input power, can be made from the application of an applied static magnetic field to a magneto-optic guide. The predicted z_0 is precisely the period in the simulation of Fig. 3, showing that a variational analysis with more degrees of freedom would not give more information in this case.

If the initial condition is $\eta_1 = \eta_2 = 1/\sqrt{2(1 - f)}$, $\theta = \pm\pi/2$, Eqs. (7) and (8) show that this initial condition is stationary. In fact, this initial condition corresponds to an exact vector soliton solution of Eq. (6), for the case $\nu = 0$, i.e., $\psi_1 = \pm i\psi_2 = 1/\sqrt{2(1 - f)}\operatorname{sech}x \exp[i(1 \mp Q_1)z]$.

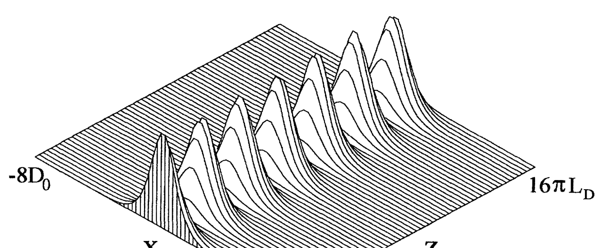

FIG. 3. Intensity plot that shows the conversion of TE to TM polarization for $Q_1 = 0.4$. Only the TE part is plotted here. The propagation is from $z = 0$ to $z = 11$ cm. The transverse direction is $-68 \le x \le 68$ μm. The numerical value of the period is $z_0 = 1.721$ cm. The period predicted variationally is $z_0 = 1.728$ cm.

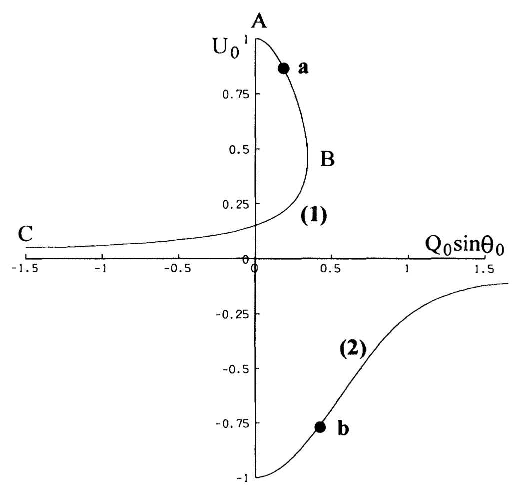

FIG. 4. Variation of stationary value U_0 with $Q_0\sin\theta_0$, for $\nu = 0.05$. a is an unstable point and b is a stable point.

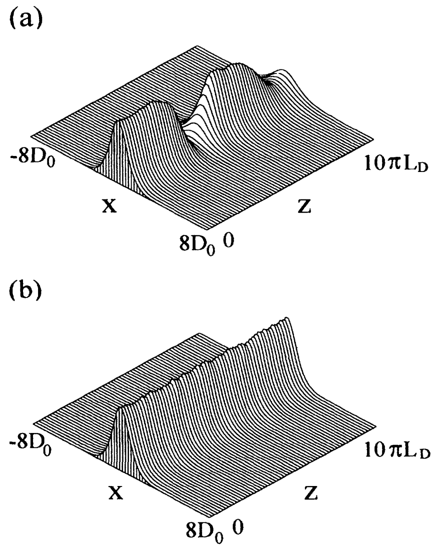

FIG. 5. Numerical simulations to check the stability regions. (a) and (b) correspond to points a and b in Fig. 4.

The stability of this vector soliton solution can be analyzed with Eqs. (7) and (8) and the analysis can also be generalized to $\nu \neq 0$.

Specifically, for the generalized case ($\nu \neq 0$), Eq. (7) is the same but (8) needs to have -4ν added to the right-hand side. The Hamiltonian density of the system is

$$H = \tfrac{4}{3} f(1 - U^2)\sin^2\theta - Q_0\sqrt{1 - U^2}\,\sin\theta + 4\nu U\,, \tag{9}$$

where $\nu' = \nu/(\eta_1^2 + \eta_2^2)$ and the dash on the ν has been dropped. Both U and θ are functions of ζ and satisfy the Hamiltonian equations

$$\partial U/\partial\zeta = \partial H/\partial\theta\,, \qquad \partial\theta/\partial\zeta = -\partial H/\partial U\,. \tag{10}$$

The vector soliton solution corresponds to a stationary state of Eq. (10). The latter occur whenever $\partial U/\partial\zeta = 0, \partial\theta/\partial\zeta = 0$ and these conditions occur at $U = U_0$, $\theta = \theta_0 = \pm\pi/2$, which is called a critical point of the system. One example of the stationary states, using Eqs. (9) and (10), is shown in Fig. 4 for $\nu = 0.05$. In the neighborhood of the critical point,

$$\frac{\partial U}{\partial\zeta} \cong \frac{\partial^2 H}{\partial\theta^2}(\theta - \theta_0) + \frac{\partial^2 H}{\partial U\partial\theta}(U - U_0)\,, \tag{11a}$$

$$\frac{\partial\theta}{\partial\zeta} \cong \frac{\partial^2 H}{\partial U\partial\theta}(\theta - \theta_0) - \frac{\partial^2 H}{\partial U^2}(U - U_0)\,. \tag{11b}$$

Assuming that perturbations in the vicinity of a critical point vary as $e^{\lambda\zeta}$, then $\lambda^2 < 0$ means stability of the (U_0, θ_0) state, while $\lambda^2 > 0$ means it is unstable, where

$$\lambda^2 = \left[\left(\frac{\partial^2 H}{\partial U\partial\theta}\right)^2 - \left(\frac{\partial^2 H}{\partial U^2}\right)\left(\frac{\partial^2 H}{\partial\theta^2}\right)\right]_{U_0,\theta_0}. \tag{12}$$

The stability condition determined from Eq. (12) shows that the AB part of curve (1), in Fig. 4, is unstable, and the BC part is stable. Curve 2 in Fig. 4 is associated with stable ($\lambda^2 < 0$) solutions. The theoretical conclusions have been checked by computer simulations, and excellent agreement is obtained. Some of the results are shown in Fig. 5. These results confirm the predicted stable or unstable behavior, lending credibility to the approximations underpinning the mathematical analysis. Finally, the deployment of magneto-optic components in nonlinear integrated optics should open up a completely new range of possibilities.

This work has been supported by the UK EPSRC.

[1] D.S. Stancil, IEEE J. Quantum Electron. **27**, 61 (1991).
[2] J.S. Aitchison, K. Al-Hemyari, C.N. Ironside, R.S. Grant, and W. Sibbett, Electron. Lett. **28**, 1879 (1992).
[3] A.D. Boardman and K. Xie, Phys. Rev. A **50**, 1851 (1994).
[4] A.D. Boardman, K. Xie, and A.A. Zharov, Phys. Rev. A **51**, 692 (1994).
[5] K.H.J. Buschow, *Ferromagnetic Materials,* edited by E.P. Wohlfarth and K.H.J. Buschow (Elsevier Science Publishers, Amsterdam, 1988).
[6] C. Paré and M. Florjanczyk, Phys. Rev. A **41**, 6287 (1990).